

# Ryk-mediated Wnt repulsion regulates posterior-directed growth of corticospinal tract

Yaobo Liu<sup>1</sup>, Jun Shi<sup>1</sup>, Chin-Chun Lu<sup>1</sup>, Zheng-Bei Wang<sup>4</sup>, Anna I Lyuksyutova<sup>2</sup>, Xue-Jun Song<sup>4</sup> & Yimin Zou<sup>1,2,3</sup>

Guidance cues along the longitudinal axis of the CNS are poorly understood. Wnt proteins attract ascending somatosensory axons to project from the spinal cord to the brain. Here we show that Wnt proteins repel corticospinal tract (CST) axons in the opposite direction. Several *Wnt* genes were found to be expressed in the mouse spinal cord gray matter, cupping the dorsal funiculus, in an anterior-to-posterior decreasing gradient along the cervical and thoracic cord. Wnts repelled CST axons in collagen gel assays through a conserved high-affinity receptor, Ryk, which is expressed in CST axons. Neonatal spinal cord secretes diffusible repellent(s) in an anterior-posterior graded fashion, with anterior cord being stronger, and the repulsive activity was blocked by antibodies to Ryk (anti-Ryk). Intrathecal injection of anti-Ryk blocked the posterior growth of CST axons. Therefore, Wnt proteins may have a general role in anterior-posterior guidance of multiple classes of axons.

In the CNS, sensory pathways form ascending fibers that relay sensory stimuli to higher brain centers. Descending fibers send motor command and regulatory signals down from the brain. In the spinal cord, somatosensory fibers project anteriorly, whereas motor pathways project posteriorly, making the spinal cord an excellent model system for studying how ascending and descending axons are guided. The mechanisms by which axons recognize the long anterior-posterior direction during initial wiring of the spinal cord have been elusive. A signaling pathway that requires Wnt and Frizzled proteins is necessary for the anterior-directed growth of commissural axons after midline crossing<sup>1</sup>.

To address the molecular mechanisms that regulate posterior-directed axon growth in the spinal cord, we studied the CST axons. CST axons originate from the frontal and sensorimotor cortices, exit the cortex, traverse the internal capsule and project posteriorly through the basal midbrain (Fig. 1a). When they reach the hindbrain, they project dorsally at the caudal medulla and cross the midline just before entering the spinal cord at postnatal day (P) 0. Most CST axons cross the midline, forming the pyramidal decussation, and enter the spinal cord, projecting posteriorly until they reach their proper anterior-posterior position. In rodents, most CST axons project posteriorly at the dorsal midline in the ventral-most portion of the dorsal funiculus (Fig. 1b)<sup>2</sup>. Leading CST axons in mice reach the caudal thoracic level at P7 (ref. 3). Although guidance and regeneration of CST axons has received much attention, the molecular guidance cues that direct the posterior growth of the CST axons in the spinal cord have not been identified.

On the basis of our knowledge of the anterior-posterior guidance of commissural axons, we studied whether Wnt proteins also regulate anterior-posterior pathfinding of CST axons. We found that several *Wnt* genes are expressed in a high-to-low gradient in the gray matter that cups the dorsal funiculus from cervical to thoracic spinal cord and

that Wnt proteins repel CST axons. The vertebrate homolog of the repulsive Wnt receptor Derailed, Ryk, is a high-affinity receptor and is expressed on CST axons<sup>4,5</sup>. Polyclonal antibodies against the ecto-domain of Ryk blocked the repulsive effect of Wnt1 and Wnt5a. The neonatal spinal cord secretes diffusible repellent(s) in a decreasing fashion along the anterior-posterior axis, and anti-Ryk blocked the repulsion. Intrathecal injection of anti-Ryk into neonatal cervical spinal cord caused a significant reduction in CST axons posterior to the injection sites and stalling of CST axons anterior to the injection sites. These results indicate that Wnt proteins may control not only the pathfinding of ascending sensory axons but also that of descending motor pathways. Therefore, Wnts may convey general directional information for axonal connections along the anterior-posterior axis in the spinal cord.

## RESULTS

### Anterior-posterior gradient of *Wnts* in neonatal spinal cord

Because CST axons project posteriorly along the dorsal funiculus of the spinal cord, we examined the expression patterns of *Wnt* genes around the dorsal funiculus. We cloned *in situ* hybridization probes for the entire family of mouse *Wnt* genes (including 19 members) and carried out *in situ* hybridization at P0 and P3 along the anterior-posterior axis. A transverse section was taken every 1.6 mm along the anterior-posterior axis of individual spinal cords and tested for expression of *Wnt* genes. We found that four *Wnt* genes are expressed in the gray matter that cups the dorsal midline and dorsal funiculus at these stages, with *Wnt1* and *Wnt5a* being expressed at a higher level (Fig. 1c,d). We noticed that the expression patterns of *Wnt1* and *Wnt5a* were not identical, demonstrating the specificity of these probes. *Wnt1* was expressed in wider areas in the dorsal half of the spinal cord

<sup>1</sup>Department of Neurobiology, Pharmacology and Physiology, <sup>2</sup>Committee on Developmental Biology and <sup>3</sup>Committee on Neurobiology, University of Chicago, Chicago, Illinois 60637, USA. <sup>4</sup>Parker College Research Institute, Dallas, Texas 75229, USA. Correspondence should be addressed to Y.Z. (yzou@bsd.uchicago.edu).

Received 18 June; accepted 15 July; published online 14 August 2005; corrected after print 14 December 2005; doi:10.1038/nn1520

**Figure 1** Anterior-posterior gradient of *Wnt* expression around the dorsal funiculus. (a) Schematic showing lateral view of CST trajectory from the frontal cortex to the spinal cord. (b) Transverse view of neonatal spinal cord showing the location of CST in the ventral-most area of the dorsal funiculus surrounded by gray matter. (c) Quantification of *in situ* signals. Digital images of *in situ* hybridizations were analyzed by NIH Image J, and the density of the positive grayscale signal was measured. The signal density of *Wnt1* and *Wnt5a* were averaged from four sets of *in situ* hybridizations from four different mice. A-P, anterior-posterior. (d) *In situ* hybridization of transverse sections along the anterior-to-posterior axis probed with *Wnt1* and *Wnt5a*, showing decreasing expression gradients of both genes along the anterior-posterior axis. *Efnb3* is expressed at the dorsal midline (arrows) at the same stages but does not show an anterior-posterior gradient. (e,f) *In situ* hybridization of transverse sections of P0 mouse spinal cord for (e) *Wnt1* and (f) *Wnt5a*. (g,h) Higher magnification of (g) *Wnt1* and (h) *Wnt5a* *in situ* hybridization, showing expression in larger (large arrowheads) and smaller (small arrowhead) cells. Scale bars, 100  $\mu$ m.

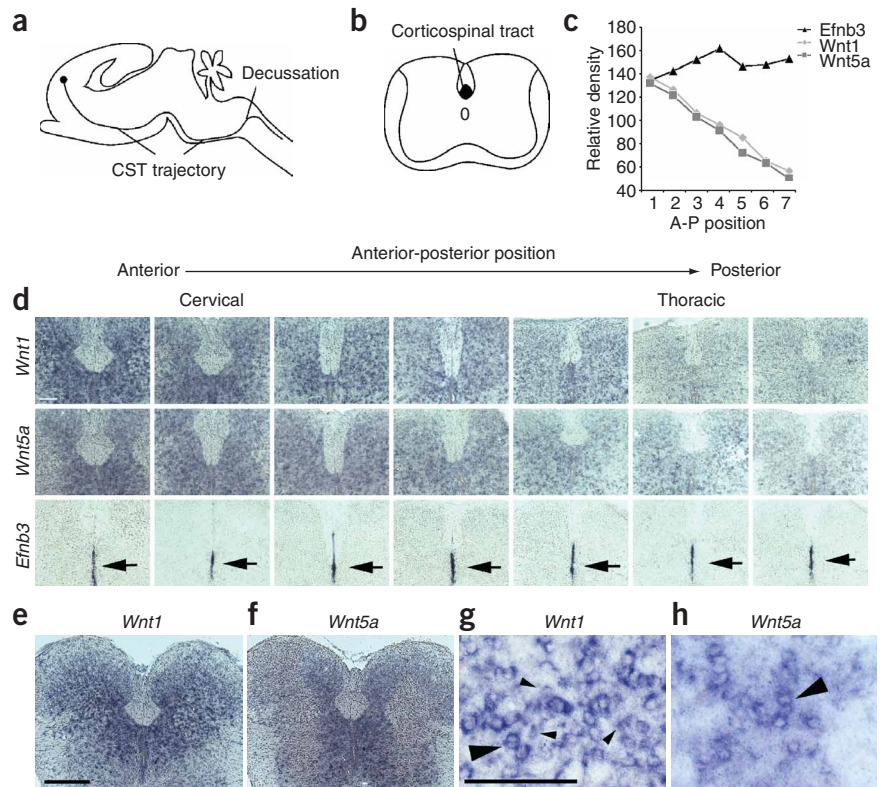


(Fig. 1e), whereas *Wnt5a* was expressed in a narrower area in the dorsal spinal cord but at higher levels in the ventral-medial domains of the spinal cord (Fig. 1f). Both *Wnt1* and *Wnt5a* were expressed in the gray matter immediately surrounding the dorsal funiculus. Although the identities of the cells expressing high amounts of *Wnt1* and *Wnt5a* are not known, *Wnt1* was expressed in both larger and smaller cells (Fig. 1g), whereas *Wnt5a* was expressed primarily in larger cells (Fig. 1h). *Wnt8a* and *Wnt9a* were expressed at much lower amounts (data not shown). Along the anterior-posterior axis, these four *Wnt* genes showed a general high-to-low gradient at cervical and thoracic spinal cord levels, although expression of the gene encoding ephrin B3 (*Efnb3*) did not show an anterior-posterior gradient (Fig. 1d). The signal intensity of *Wnts* was quantified from four sets of *in situ* experiments (Fig. 1c). CST axons arrive at the medulla–spinal cord junction at P0 and during the first few days of postnatal life. Pioneering CST axons enter the cervical spinal cord and reach the posterior thoracic levels only at P5 (ref. 3). Therefore, CST axons pathfind within the *Wnt1* and *Wnt5a* gradients inside the spinal cord.

### Wnt proteins repel motor cortical axons

To test whether Wnts can guide CST axons, we carried out explant cultures to evaluate the function of Wnt proteins on the motor cortical axons in collagen gel assays (Fig. 2). P0 brains were dissected out and sliced with a tissue chopper (see Supplementary Fig. 1 online). Layer 5 cortical explants were dissected from the frontal and sensorimotor cortical regions and were cultured in collagen for 60 h (Supplementary Fig. 1). To ensure that the cultures were consistent and that only motor cortical explants were cultured, only three explants were dissected from each side of the cortical slices and only two slices (each was 250  $\mu$ m thick) from the correct areas were used from each brain.

To test the function of Wnts, COS7 cells were transfected with Wnt expression constructs, aggregated into cell clumps and positioned next to the cortical explants from P0 motor cortex (Fig. 2a). We found that *Wnt1* and *Wnt5a* potentially inhibited the outgrowth of axons from the

motor cortex in these assays, indicating that CST axons might respond to Wnt proteins as they pathfind along the spinal cord *in vivo*. Very few axons grew out in the collagen gel, and the axon length was markedly reduced as well. To address the possibility that the cell aggregates secreted excessive amounts of *Wnt1* and *Wnt5a* proteins, preventing axons from growing out of the explants, we diluted the transfected COS cells with untransfected COS cells and began to observe strong repulsion by cells expressing *Wnt1* and *Wnt5a* (Fig. 2b).

Results were quantified from eight explants for each set of experiments (Fig. 2c,d and Supplementary Fig. 2), and the means ( $\pm$  s.d.) of five sets of experiments were calculated. We tested the function of *Wnt1* and *Wnt5a* on E18.5 cortical axons and found that in contrast to P0, *Wnt1* and *Wnt5a* did not repel motor cortical axons from E18.5 (data not shown). CST axons reach the spinal cord at P0. At E18.5, the CST axons are still in the midbrain and the hindbrain. The timing of *Wnt1* responsiveness is consistent with its potential role in pathfinding for CST axons as they enter the spinal cord.

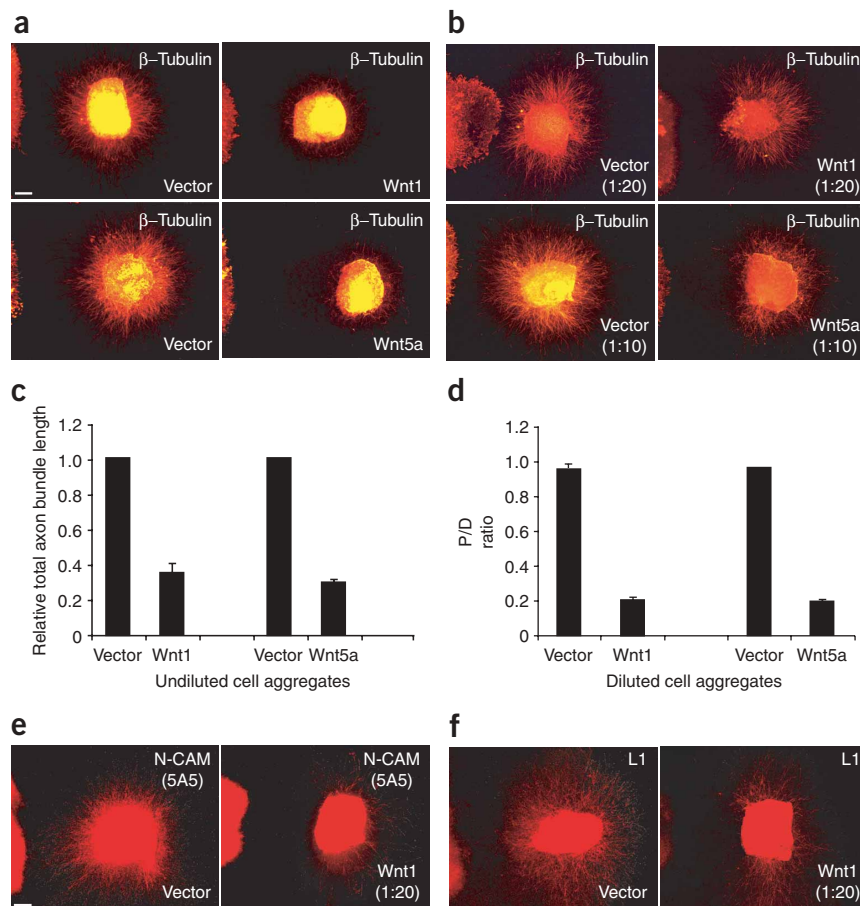
These long axons that were growing out in the collagen gel and were repelled by Wnts stained positively for two CST markers, a monoclonal antibody to neural cell adhesion molecule (N-CAM), 5A5 (ref. 6; Fig. 2e), and polyclonal antibodies to L1 (anti-L1; Fig. 2f). Therefore, these axons are CST axons, and the markers did not change after coculturing with *Wnt1*-expressing COS cell aggregates.

### Ryk is expressed in CST axons

Axon guidance molecules are often bifunctional, attracting some axons but repelling others, depending on the responding neurons. Vertebrate spinal cord commissural axons are attracted by Wnts<sup>1</sup>, whereas motor cortical axons are repelled by Wnts. In *Drosophila melanogaster*, *Wnt5* has a repulsive role in pathway selection before midline crossing<sup>4</sup>. This repulsion is mediated by a Wnt receptor named Derailed through direct binding and is independent of Frizzled<sup>4</sup>. Therefore, the vertebrate

**Figure 2** Wnts repel motor cortical axons.

(a) Wnt1- or Wnt5a-expressing COS cell aggregates (undiluted) showed strong inhibition of the growth of PO layer 5 frontal cortical axons, stained with  $\beta$ -tubulin antibodies. (b) Axons from layer 5 explants of PO frontal cortex were repelled by Wnt1- or Wnt5a-transfected COS cells (diluted to show repulsion: Wnt1, 1:20; Wnt5a, 1:10). (c) Quantification of the inhibitory effects of Wnts. The relative total axon bundle lengths were obtained by the ratio of total axons from explants exposed to Wnt-transfected COS cell aggregates over explants exposed to vector-transfected COS cell aggregates. (d) Quantification of Wnt repulsion of motor cortical axons. The repulsion was measured by the proximal/distal (P/D) ratio: ratio of axon length in the proximal quadrant versus that in the distal quadrant. (e) Axons from layer 5 frontal cortical explants stained positively with a CST axon marker, 5A5 (N-CAM<sup>6</sup>) and were repelled by Wnt1-expressing COS cell aggregates (diluted 1:20 with untransfected cells). (f) Axons from layer 5 frontal cortical explants stained positively with another CST marker, L1, and were repelled by Wnt1-expressing COS cell aggregates (diluted 1:20). Scale bars, 100  $\mu$ m.



homolog of Derailed, Ryk, is a candidate receptor for Wnt-mediated repulsion of CST axons.

We first generated an *in situ* probe for Ryk and carried out *in situ* hybridization. Ryk was expressed in layers 5 and 6 of the frontal and sensorimotor cortices at P0 as well as in layers 2 and 3 (Fig. 3a,b). At E18.5, Ryk was expressed in layers 2 and 3 but was barely detectable in layers 5 and 6, and the signal was weaker than that of P0 (Fig. 3a,b). This correlates with the observation that E18.5 cortical axons are not repelled by Wnts, whereas P0 axons are robustly repelled. We then generated polyclonal antibodies to the extracellular domain of Ryk and further confirmed that Ryk protein is present in layer 5/6 cells in P0 motor cortex but not in layers 5/6 in E18.5 motor cortex (Fig. 3c). At E18.5, however, only layer 2/3 cells expressed Ryk protein (Fig. 3c). In sagittal sections, the pyramidal tracts showed highly specific Ryk staining. At P0, CST axons have just arrived at the medulla–spinal cord junction, and Ryk expression was stronger at the distal end of the tracts (Fig. 3d). At P5, when the CST axons have already entered the spinal cord and have started pathfinding in the dorsal funiculus, Ryk expression was higher in general (Fig. 3d). Anti-Ryk stained the CST axons specifically in the dorsal funiculus (Fig. 3d). Anti-L1 staining was carried out to show the trajectory of the CST. The L1 signal was weaker in the distal end of the CST than in the proximal end (Fig. 3d), suggesting that L1 is expressed in broader areas in the brain than Ryk. The CST axons that form the pyramidal decussation (Fig. 3d) and the pyramidal tracts in the dorsal funiculus of the spinal cord (Fig. 3e) expressed high amounts of Ryk. Therefore, Ryk is expressed in CST axons at the appropriate time to mediate Wnt repulsion and may be involved in the descending growth of CST axons within the spinal cord.

To test whether Ryk is a vertebrate receptor for Wnts, we generated Wnt1–alkaline phosphatase (AP) fusion proteins and carried out binding assays with COS cells transfected with Ryk. We found that Wnt1 can bind to Ryk, as well as to Frizzled (Fzd3) as a control

(Fig. 3f). To assess the affinity of the Wnt-Ryk interaction, we quantified binding and found that the  $K_d$  for Wnt1-AP to Ryk was 7.89 nM. In parallel experiments, the affinity of Wnt1-AP to Fzd3 was 53.91 nM (Fig. 3f). Therefore, Ryk is a high-affinity Wnt receptor.

To test whether Ryk is expressed in the motor cortical explants shown in Figure 2 and whether Wnts affect the expression of this receptor by changing cell fate, we stained explants exposed to Wnt1-expressing cell aggregates with anti-Ryk (Fig. 3g). The cortical explants that were exposed to Wnt1 still expressed similar amounts of Ryk protein, and the Ryk-positive axons were actively repelled by Wnt1 cell aggregates. Many axons were deflected away from the Wnt1 cell clumps (arrows in Fig. 3g).

#### Anti-Ryk blocks the repulsion by Wnts

To determine whether Ryk is involved in mediating Wnt repulsion in vertebrate axons and whether it functions as a Wnt receptor, we used polyclonal antibodies generated to the ectodomain of Ryk (anti-Ryk) and tested whether anti-Ryk could block the repulsion by Wnts in collagen gel assays. We found that addition of purified anti-Ryk in collagen gel assays blocked the repulsive effects of Wnt proteins, whereas the preimmune control did not (Fig. 4a,b). In the presence of preimmune serum, motor cortical axons tended to grow away from the point source of Wnt1 and Wnt5a. When anti-Ryk was included, motor cortical axons were no longer repelled. Therefore, Ryk is required for mediating Wnt repulsion of CST axons in collagen gel assays. Results (Fig. 4a,b) were quantified and averaged from five sets of experiments (Fig. 4g). In each set, eight explants were included for each of the eight conditions (vector + preimmune, Wnt1 + preimmune,

vector + anti-Ryk, Wnt1 + anti-Ryk, vector + preimmune, Wnt5a + preimmune, vector + anti-Ryk, Wnt5a + anti-Ryk).

To test whether blocking of Wnt repulsion by anti-Ryk is specific, we tested whether anti-Ryk can block the repulsion of other repellents, such as the slit proteins. In the presence of preimmune serum, Slit2 can repel postcrossing commissural axons in a collagen gel assay<sup>7</sup>. In the presence of anti-Ryk, Slit2 was still able to repel postcrossing commissural axons (Fig. 4c,e; two sets of experiments were averaged).

Multiple explants were included in each of the four conditions (vector + preimmune,  $n = 11$ ; Slit2 + preimmune,  $n = 8$ ; vector + anti-Ryk,  $n = 8$ ; Slit2 + anti-Ryk,  $n = 17$ ).

To test further whether anti-Ryk specifically blocks Wnt-mediated repulsion of CST axons, we tested whether anti-Ryk can block Wnt-mediated attraction. Wnt4 can attract postcrossing commissural axons<sup>1</sup>. When anti-Ryk was added to the culture, commissural axons were still attracted by Wnt4-expressing COS cell aggregates

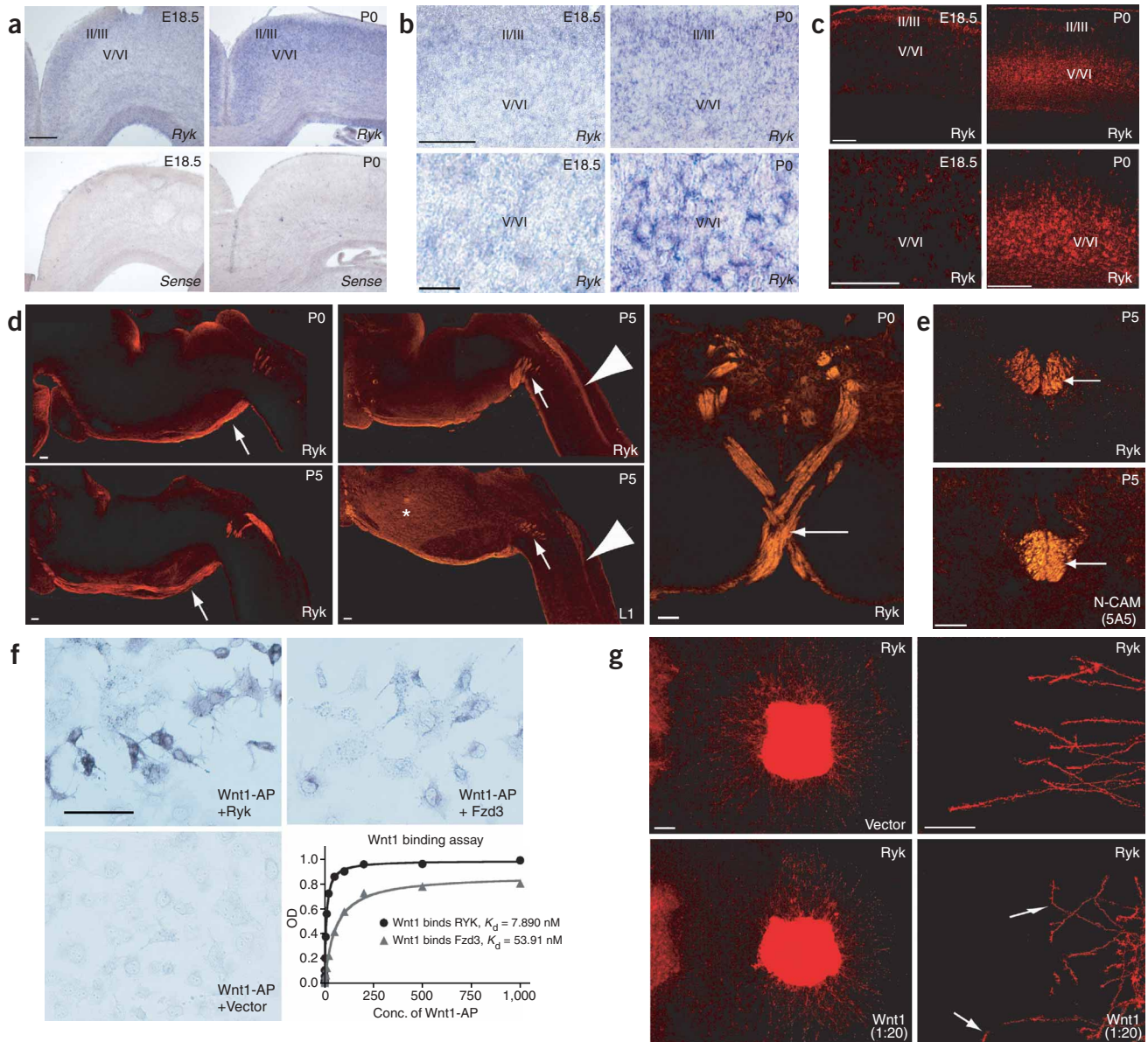


(Fig. 4d,f). Multiple explants were tested in each of the four conditions (vector + preimmune,  $n = 7$ ; Wnt4 + preimmune,  $n = 6$ ; vector + anti-Ryk,  $n = 7$ ; Wnt4 + anti-Ryk,  $n = 7$ ). Therefore, anti-Ryk does not block all Wnt-mediated effects on axons, documenting the specificity of anti-Ryk in blocking Wnt-mediated repulsion of CST axons.

#### Anterior-posterior graded chemorepulsion by neonatal cord

As Wnts are diffusible guidance cues and are expressed in an anterior-posterior graded fashion, it is possible that such an anterior-posterior gradient provides directional information for CST axons along the longitudinal axis of the spinal cord. We carried out cocultures of motor cortical axons with neonatal spinal cord tissue in collagen gel and found that neonatal spinal cord secretes diffusible repellents that repel CST axons. We first collected vibratome sections (slices) along the anterior-posterior axis of the spinal cord (Fig. 5a) and then cut the dorsal spinal cord areas where the CST axons pathfind and placed dorsal spinal cord tissue pieces of equal size next to the cortical explants (Fig. 5b). Anterior spinal cord tissue (from the cervical regions) showed stronger repulsion than did posterior spinal cord tissue (from the thoracic regions). Along the anterior-posterior axis (positions 1, 2 and 3), there was a decreasing gradient of repulsive effect (Fig. 5b). To investigate further the identity of the repellents, we tested whether anti-Ryk can block the spinal cord-derived repellent(s) and found that in the presence of anti-Ryk, CST axons showed radial growth, whereas in the preimmune control, CST axons were repelled by neonatal spinal cord in an anterior-posterior graded fashion (Fig. 5b,c). The graded repulsive effect of neonatal spinal cord is likely due to the graded distribution of the Wnt proteins, which may

provide directional information for cortical motor axons to grow posteriorly along the spinal cord.

#### Anti-Ryk blocked posterior growth of CST axons

To test whether a Wnt-Ryk interaction is required for the anterior-posterior guidance of CST axons *in vivo*, we injected purified anti-Ryk into cervical spinal cord. Mice were injected with 50  $\mu\text{g/ml}$  antibodies or preimmune control on P1 and P3 and were killed on P5 and fixed by cardiac perfusion. Along the anterior-posterior axis, sections were taken every 800  $\mu\text{m}$  and were analyzed by immunostaining with anti-N-CAM monoclonal antibody 5A5, a CST marker. Mice injected with anti-Ryk showed a marked reduction in CST fibers posterior to the injection site but an increase in CST areas anterior to the injection sites, whereas mice injected with the vehicle control, artificial cerebrospinal fluid (ACSF) or with preimmune serum showed normal CST areas (Fig. 6a). Similar results were obtained in six different sets of mice. Each set included ACSF-, preimmune- and anti-Ryk-injected mice. CST areas were quantified from four spinal cords (Fig. 6b). CST axon areas were larger anterior to the injection sites, suggesting that the CST fibers may be stalling anterior to the injection site.

To characterize further the CST axon projections after anti-Ryk injection, we did DiI tracing and viewed the CST axons along the anterior-posterior longitudinal axis. Small DiI crystals were planted into the medulla-spinal cord junction at the pyramidal decussation, and DiI was allowed to diffuse for 6 weeks. Sagittal sections were taken at a thickness of 10  $\mu\text{m}$ . The entire CST axon bundle was usually contained in three consecutive sagittal sections. Therefore, we evaluated the entire CST axon bundle by looking at these three sections (Fig. 6c,d). CST axons in mice injected with anti-Ryk were substantially reduced posterior to the injection area as compared with those injected with vehicle (ACSF) or preimmune serum. CST axon bundles anterior to the injection area appeared wider and less compact as compared with vehicle and preimmune controls (Fig. 6d). A total of five sets of mice were analyzed for each treatment (ACSF, preimmune or anti-Ryk injections) and yielded similar results. The DiI tracing results are consistent with the observation of CST staining in serial transverse sections (Fig. 6a,b). A small amount of purified antibodies (1  $\mu\text{l}$ ) was injected intrathecally (between the dura and spinal cord tissue), which should not damage the spinal cord tissue. In fact, the control vehicle and

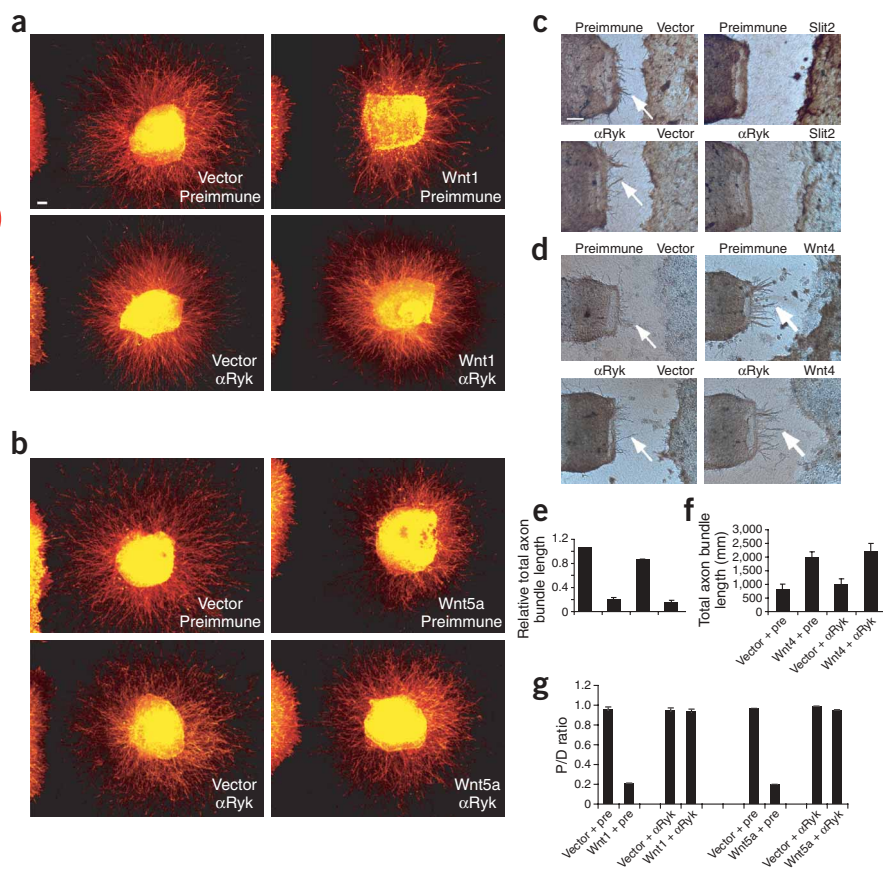
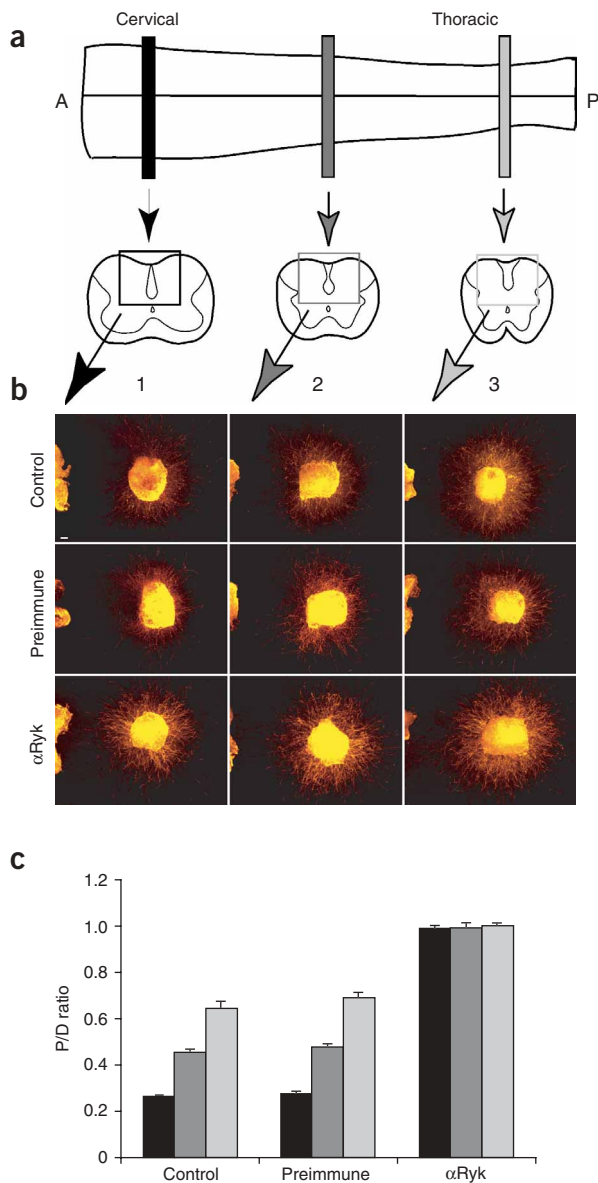


**Figure 4** Ryk is required for Wnt1 and Wnt5a repulsion. (a,b) Anti-Ryk ( $\alpha$ Ryk; 50  $\mu\text{g/ml}$ ) blocked repulsion of P0 layer 5 motor cortical axons by (a) Wnt1 and (b) Wnt5a. (c) Anti-Ryk (50  $\mu\text{g/ml}$ ) did not block repulsion of postcrossing spinal cord commissural axons by Slit2. (d) Anti-Ryk (50  $\mu\text{g/ml}$ ) did not block the attraction of crossing commissural axons by Wnt4. (e) Quantification of Slit2 repulsion of postcrossing commissural axons in the presence and absence of anti-Ryk antibodies. (f) Quantification of Wnt4 attraction of postcrossing commissural axons in the presence and absence of anti-Ryk. (g) Quantification of Wnt1 and Wnt5a effects on P0 layer 5 motor cortical axons in the presence and absence of anti-Ryk. Scale bars, 100  $\mu\text{m}$ .



preimmune serum injections did not cause any defects or damage. Taken together, our results indicate that Wnt-Ryk signaling is required for posterior growth of CST axons within the dorsal funiculus of the neonatal rodent spinal cord *in vivo*.

## DISCUSSION

CST axons are one of the major descending motor pathways and control voluntary body movement and fine motor functions of the limbs. They are some of the longest axons in the human or animal body and connect the motor cortex to motor circuits at various anterior-posterior positions in the spinal cord. The development and regeneration of the CST have been studied intensely, but very little is known about the guidance cues that are involved. Until now, only a couple of molecules have been found to be important in regulating the pathfinding of CST axons from the brain to the spinal cord. Neural cell adhesion molecules of the immunoglobulin superfamily (IgCAMs) have been implicated in both the fasciculation and guidance of axons. L1, a member of the IgCAM family, has been implicated in many neural processes and is expressed widely in the embryonic and adult nervous

**Figure 5** Neonatal spinal cord secretes diffusible repellent(s) in an anterior-posterior graded fashion, which can be blocked by anti-Ryk. **(a)** Diagram showing the three anterior-posterior positions where neonatal (P0) mouse spinal cord slices were cut by tissue chopper. Equal-sized dorsal spinal cord areas surrounding the dorsal funiculus were dissected out and positioned next to the neonatal (P0) cortical explants from the same mouse. **(b)** The anterior-posterior graded repulsive effects of neonatal spinal cord (anterior-posterior positions 1, 2, 3) can be blocked by anti-Ryk. **(c)** Quantification of proximal/distal ratios. The results were averaged from three sets of assays. In each set, three anterior-posterior positions (1, 2, 3) were tested in three conditions: control, preimmune serum and anti-Ryk. For each condition and each anterior-posterior position, two cortical explants were tested and averaged in each set. Scale bar, 100  $\mu$ m.

systems<sup>8</sup>. L1 function is necessary for the guidance of corticospinal axons across the pyramidal decussation in mice. Although the pathway to the caudal medulla seems normal, a substantial proportion of axons fail to cross the midline to the opposite dorsal column in L1-deficient mice<sup>8</sup>. L1 is a component of the Sema3A receptor complex, and L1 mutations may disrupt Sema3A signaling, leading to guidance errors<sup>9</sup>. The receptor tyrosine kinase EphA4 mediates midline pathfinding of CST axons. In mice with null mutations in the gene encoding EphA4, anatomical studies and anterograde tracing experiments show major disruptions of the CST within the medulla and spinal cord in the null mutant mice, including aberrant recrossing of the dorsal midline, although CST pathfinding in the forebrain and midbrain is normal<sup>10</sup>. A recent study identified a gene, *Bcl11b* (also known as *Ctip2*), which encodes a transcription factor, that is critical for the development of axonal projections of corticospinal motor neurons to the spinal cord *in vivo*<sup>11</sup>. In *Bcl11b*<sup>-/-</sup> mice, CST axons lack fasciculation in the sub-cerebral projections in the internal capsule after the postnatal stage.

A major question of CST guidance is how the corticospinal motor axons pathfind along the anterior-posterior direction in the postnatal spinal cord. The directional cue has remained unknown. In this study, we found that several Wnt proteins form a high-to-low anterior-posterior gradient in the cervical and thoracic spinal cord during the first week of postnatal life of mice, when CST axons first enter the spinal cord and project posteriorly. These Wnt proteins are potent repellents of CST axons, and this repulsion is mediated by a conserved receptor, Ryk, a protein tyrosine kinase-like transmembrane protein. Neonatal spinal cord secreted diffusible repellents in an anterior-posterior graded fashion, and this repulsion was blocked by anti-Ryk. Blocking Ryk in developing spinal cord led to a marked reduction in CST fiber formation posterior to the injection sites and to the accumulation of CST axons anterior to the injection sites *in vivo*, suggesting that the Wnt proteins are essential for the proper development of CST axons.

Axon connections along the anterior-posterior (rostral-caudal) axis are an important aspect of nervous system wiring. Much attention has been devoted to understanding axon connections along the dorsal-ventral axis, such as growing toward and away from the midline<sup>12</sup>. Very little is known about the molecular guidance cues along the anterior-posterior axis in any animal system. Wnts control the anterior turning of postcrossing commissural axons at the ventral midline of midgestation embryos<sup>1</sup>. Our current study documents the function of Wnt gradients in guiding the posterior growth of CST axons at the neonatal stage while they are pathfinding at the cervical and thoracic levels. We thus propose that Wnts may form gradients to regulate axon pathfinding of both ascending sensory axons, such as the spinal cord commissural axons<sup>1</sup>, and descending motor axons, such as the CST axons, and that Wnt family proteins are potentially general anterior-posterior guidance signals for spinal cord axons.

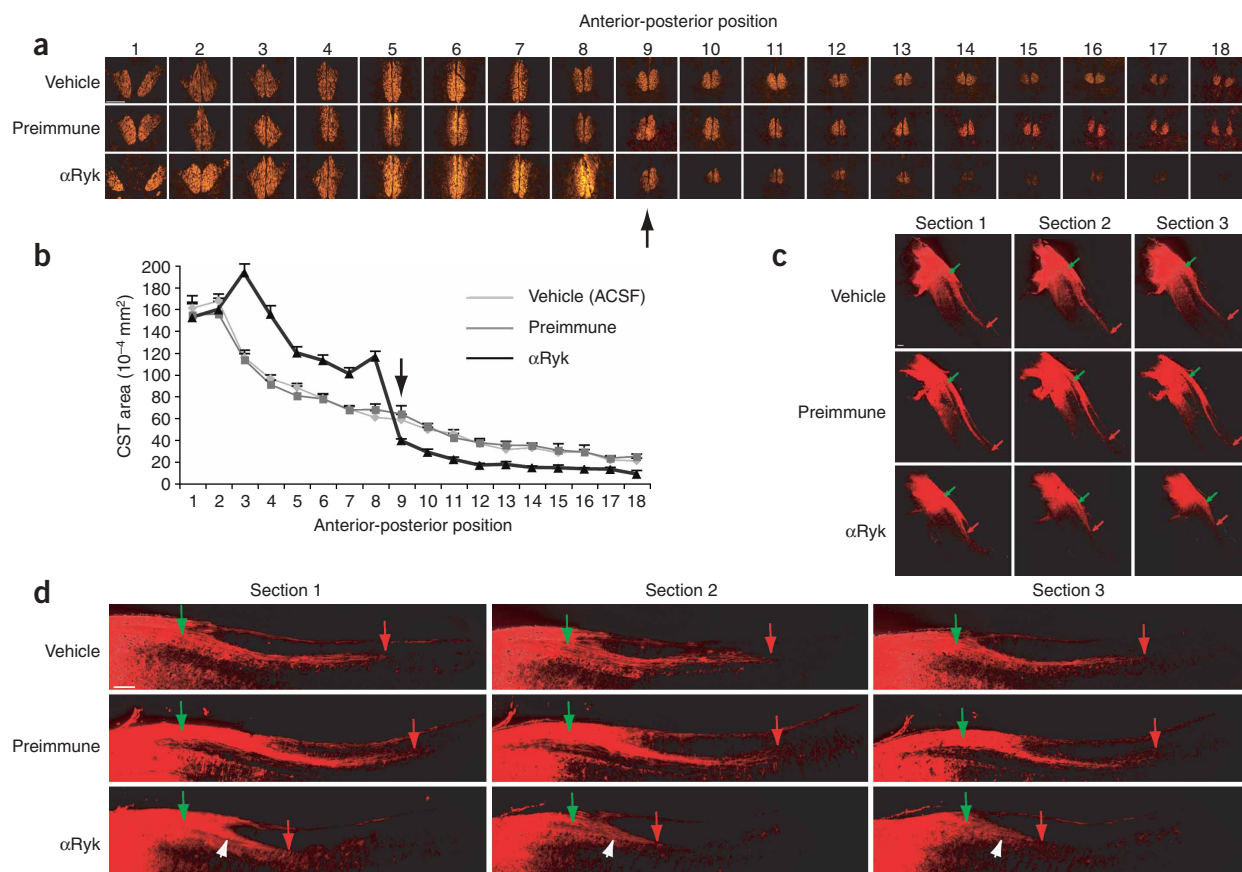


**Figure 6** Anti-Ryk blocked posterior growth of CST axons *in vivo*. **(a)** Immunostaining with 5A5 showing that the CST areas are reduced in size and intensity posterior to the injection sites but are enlarged anterior to the injection sites (arrow) in mice injected with anti-Ryk. **(b)** Quantification of CST areas. CST areas in antibody-injected mice anterior to the injection site are larger than in controls, particularly in anterior-posterior position 8, suggesting that CST axons were stalling anterior to the injection site, anterior-posterior position 9 (arrow). **(c)** Serial sagittal sections (sections 1–3) of P5 mouse showing the entire CST bundles in mice injected with vehicle, preimmune serum or anti-Ryk. Green arrows indicate the same anterior position that is consistent in all mice along the anterior-posterior axis as a reference point. Red arrows indicate the posterior end of the Dil labeling that is clearly visible. The antibody-injected mice showed markedly reduced growth of CST axons, similar to the results shown in **a** in serial transverse sections. **(d)** Higher-magnification pictures of **c**, showing details of Dil tracing of the CST axons. CST axons failed to grow efficiently posteriorly when injected with anti-Ryk. CST bundles with anti-Ryk appear wider and less compact (white arrows). Red arrows, approximate injection sites. Scale bars: 100  $\mu\text{m}$  in **a**, 1,400  $\mu\text{m}$  in **c,d**.

The trajectory of CST axons is quite complex, particularly before they reach the spinal cord (Fig. 1a). Therefore, it is conceivable that multiple guidance cues may be involved in defining their pathways. At P0, CST axons were strongly repelled by Wnts, but E18.5 CST axons were not repelled. The onset of Wnt responsiveness coincides with the upregulation of Ryk immunoreactivity in the deep layers of frontal motor cortex (Fig. 3c) and the enrichment of Ryk protein at the pyramidal decussation (Fig. 3d). Therefore, Wnts probably begin to repel CST axons once they have reached the medulla–spinal cord junction, and the Wnt expression gradient along the anterior-posterior axis provides directionality for CST axons to grow posteriorly. *Wnt1* and *Wnt5a* transcripts were expressed at even higher amounts in the medulla anterior to the decussation (data not shown). It is possible that Wnt repulsion is involved in the posterior turning at the decussation and in the subsequent descending growth of CST axons in the spinal cord. It is technically challenging to deliver antibodies reliably to the pyramidal decussation in neonatal mice to test the role of Ryk in the initial posterior turning. Intrathecal injection could only deliver anti-Ryk between the joint of C4 and C5 because of the small size of neonatal mice. Injection of anti-Ryk into the upper neonatal cervical spinal cord did, however, result in stalling of CST axons and in the reduction of

CST fibers in the dorsal funiculus, supporting the role of Wnts in CST guidance along the anterior-posterior axis inside the spinal cord *in vivo*. Anti-Ryk injection resulted primarily in the stalling of CST axons (Fig. 6). Posterior to the injection site, CST areas were greatly reduced, whereas CST axons appeared widened and less compact anterior to the injection site. No other defects, such as random overshooting or abnormal branching were observed. It is possible that other guidance molecules are involved in restricting the CST fibers within the ventral areas of the dorsal funiculus and that the primary function of Wnts is to guide the CST axons to grow posteriorly. The conventional *Ryk* knockout mice typically die at the day of birth and display severe patterning defects<sup>5</sup>. The *Ryk* small interfering RNA transgenic mice also typically die at birth<sup>13</sup>. Therefore, phenotypic analyses of postnatal CST axon guidance in these mice would be complicated by issues of early developmental defects and potentially by other functions of *Ryk*.

Wnts are recently identified axon guidance molecules and seem to function as both attractants and repellents. Wnts attract postcrossing commissural axons in a *Fzd3*-dependent manner<sup>1</sup>. *Ryk* may be required for *Wnt1*- and *Wnt3a*-stimulated neurite outgrowth from dorsal root ganglion<sup>13</sup>. In the *D. melanogaster* midline, a subset of *derailed*-expressing commissural axons was found to be repelled by *Wnt5*

(ref. 4). We show here direct evidence that vertebrate CST axons are repelled by Wnts (Wnt1 and Wnt5a) and that the repulsion is mediated by the vertebrate homolog of Derailed, Ryk<sup>5</sup>. In characterizing the Wnt-Frizzled and Wnt-Ryk biochemical interaction, we found that Sfrp2 (secreted frizzle-related sequence protein 2) can block Wnt-Frizzled binding but cannot block Wnt-Ryk binding and, conversely, Ryk antibodies (to the WIF domain) can block Wnt-Ryk binding but cannot block Wnt-Frizzled binding (data not shown). We found that Sfrp2 did not block the repulsion of CST axons by Wnts, suggesting that Frizzleds are not required to mediate Wnt repulsion of CST axons (data not shown). Therefore, Frizzleds have so far been found to mediate only attraction, and Ryk/Derailed is involved in repulsion and perhaps also attraction<sup>13</sup>. We also tested whether other Wnts have similar effects on CST axon growth in collagen gel assays and found that Wnt4, Wnt6 and Wnt7b did not have any effect (data not shown). These Wnts that had no effect on CST axons were found to attract the postcrossing commissural axons<sup>1</sup>. Therefore, there seems to be specificity of Wnts in regulating different classes of axons, which may be determined by the binding specificity of Wnts to different classes of receptors, Ryk or Frizzleds. More and more studies document the evidence of involvement of Wnts in axon guidance, which will eventually lead to a better understanding of the specificity of Wnts and their effects by means of their cognate receptors.

## METHODS

***In situ* hybridization and immunohistochemistry.** Specific *in situ* probes for the entire mouse Wnt gene family, *Wnt1*, *Wnt2*, *Wnt2b*, *Wnt3*, *Wnt3a*, *Wnt4*, *Wnt5a*, *Wnt5b*, *Wnt6*, *Wnt7a*, *Wnt7b*, *Wnt8a*, *Wnt8b*, *Wnt9a*, *Wnt9b*, *Wnt10a*, *Wnt10b*, *Wnt11* and *Wnt16*, were cloned by PCR with reverse transcription (RT-PCR) from various stages of mouse embryos and adult mouse brains into the pCRII vector (Invitrogen). Sections of neonatal spinal cords were collected every 1.6 mm along the anterior-posterior axis for evaluation of the expression of all *Wnt* genes (19 members) along the anterior-posterior axis. The *Ryk in situ* probe was cloned by RT-PCR from mouse E13.5 cDNA. The 1-kb probe included 500 nucleotides of 3' untranslated region and 500 nucleotides of the coding region at the carboxy terminus. Fetal or neonatal mouse brains were sectioned for analysis of *Ryk* expression. *In situ* hybridizations were carried out as described<sup>14</sup>.

Polyclonal anti-Ryk antibodies were generated against the ectodomain of Ryk, amino acids 90–183, fused with maltose binding protein, which was purified and injected into rabbits<sup>15</sup>. Fetal and neonatal brains were sectioned for analyses of Ryk distribution in CST axons by use of purified anti-Ryk. The N-CAM antibody 5A5 was purchased from the Developmental Studies Hybridoma Bank. Spinal cord sections were taken every 800  $\mu$ m along the anterior-posterior axis to evaluate CST axon projections using 5A5 as a CST marker<sup>6</sup>. Immunohistochemistry was carried out as described<sup>16</sup>.

**Wnt-receptor binding assays.** Wnt-receptor binding assays were carried out as described<sup>17</sup>, with slight modification. HEK293 cells were transfected with a Wnt1-AP fusion construct using FuGENE6. Cells were switched to Opti-MEM when they grew to 80–90% confluence after transfection. The medium was conditioned for an additional 48 h and concentrated 20-fold using Centrprep YM-30 (Millipore Corp) at 4 °C. COS cells transfected with a Ryk full-length expression construct, cloned by RT-PCR from adult mouse cDNA, or a Fzd3 full-length expression construct, cloned by RT-PCR from E11.5 mouse cDNA, were grown on glass coverslips, rinsed once with binding buffer (Hanks' balanced salt solution with 0.5 mg/ml BSA, 0.1% NaN<sub>3</sub> and 20 mM HEPES, pH 7.0), incubated with Wnt1-AP-containing conditioned medium for 75 min at room temperature and washed six times in binding buffer at room temperature for a total of 45 min. Cells were then fixed for 1 min in 60% acetone and 3% formaldehyde in 20 mM HEPES (pH 7.0), washed three times in 150 mM NaCl and 20 mM HEPES (pH 7.0) and heated at 65 °C for 2 h. After being washed once with alkaline phosphatase buffer (0.1 M Tris-HCl, pH 9.5; 0.1 M NaCl; 5 mM MgCl<sub>2</sub>), cells were stained at room temperature overnight with 5-bromo-4-chloro-3-indolyl-phosphate (165  $\mu$ g/ml)/nitroblue tetrazolium (330  $\mu$ g/ml) in alkaline phosphatase buffer for color detection.

**Explant assays.** Whole brains from P0 mice were dissected out and kept immersed in L15 medium. Unwanted portions (brain stem and hindbrain) were trimmed with fine forceps and razor blade knives. The forebrain was sectioned in the coronal plane with a McILWAIN tissue chopper into cortical slices (250  $\mu$ m thick), which were transferred to fresh L15 medium. Layer 5 cortical explants were dissected out from cortical slices containing frontal and sensorimotor cortices with sharp tungsten needles. COS7 cells transfected with Wnt1 or Wnt5a expression constructs or with vector only were made into hanging drops and were cut into aggregates. Different COS cell aggregates and motor cortical explants were embedded in collagen matrix and were cultured in 10% FBS MEM at 37 °C in 5% CO<sub>2</sub> for 60 h. For antibody blocking assays, purified postimmune Ryk antibody or preimmune control serum was added in culture medium with a final concentration 50  $\mu$ g/ml. After culture, motor cortical explants were fixed, and whole-mount immunofluorescence was done with the monoclonal  $\beta$ -tubulin antibody E7 or with 5A5. Using NIH Image J, the total length of axons emerging from explants or the length of axons emerging from the distal and proximate sides of explants toward COS cell aggregates was measured, which was then converted into proximal/distal ratios. In every experiment, the average relative outgrowth or proximal/distal ratio under each condition (exposed to Wnts or vector control or with preimmune or postimmune serum) was measured from eight explants. The means of five experiments were calculated.

For spinal cord tissue and cortical explant coculture experiments, cervical and thoracic spinal cords were cut into three parts of equal length along the anterior-posterior axis, using a McILWAIN tissue chopper. Each part was sectioned in the coronal plane into slices of spinal cord (250  $\mu$ m thick). These slices were transferred to fresh L15 medium and the dorsal part of the spinal cord was dissected out with sharp needles.

Postcrossing commissural axon assays were carried out as previously described<sup>7</sup>.

**Intrathecal injection.** Preimmune serum and postimmune anti-Ryk were purified with protein A-G beads and were dialyzed into ACSF. Newborn ICR mice were briefly anesthetized with halothane (1–3%). An incision was made in the midline of the spine between the joint of the C4–C5 vertebrae for injection into the spinal cord at the cervical C1–C2 level. The thin muscles were separated slightly so that the joints of the vertebrae could be easily identified. Then a fine, blunt stainless steel needle with a syringe filled with purified serum (50  $\mu$ g/ml) in ACSF was inserted approximately 3 mm into the vertebrae in a rostral direction. The reagent (1  $\mu$ l) was injected into each mouse, and the muscles and skin were sutured. Intrathecal administrations were made on P1 and P3 with the same protocol. On P5, mice were killed and fixed with cardiac perfusion of 4% paraformaldehyde before collecting tissues. Four sets of experiments (ACSF, preimmune and postimmune) were quantified (Fig. 6b). The intrathecal injection experiments were carried out in agreement with the regulations of the ethics committee of the International Association for the Study of Pain and were approved by the Parker Research Institute Animal Care and Use Committee. Serial sections were obtained along the anterior-posterior axis, and the CST axons were examined by immunohistochemistry with 5A5 monoclonal antibody.

**CST tracing.** Anterograde DiI tracing of CST axons was done in fixed P5 tissue including whole brain and spinal cord. Small DiI crystals were put in the junction area between the hindbrain and cervical spinal cord, where CST axons form the pyramidal decussation. DiI-labeled tissue in 4% paraformaldehyde was left at 4 °C for 6 weeks. After embedding, DiI-labeled spinal cord tissues were immediately sectioned sagittally at a thickness of 10  $\mu$ m and were analyzed. All sections containing CST bundles were collected and compared as shown (Fig. 6c,d). Five sets of intrathecal injection and DiI tracing experiments were carried out, yielding similar results.

All animal experiments were approved by the University of Chicago Institutional Animal Care and Use Committee.

**Accession codes.** BIND identifiers (<http://bind.ca>): 315474 and 315475.

*Note: Supplementary information is available on the Nature Neuroscience website.*



## ACKNOWLEDGMENTS

This work was supported by a Career Development Award from the Schweppe Foundation, Robert Packard ALS Center at Johns Hopkins University, the Brain Research Foundation and the Jack Miller Peripheral Neuropathy Center at the University of Chicago. We thank laboratory members L. King, A. Wolf, A. Schmitt, R. Sherman, J. Chen and A. Fenstermaker for comments and N. Milanesio for help with probes and reagents. We thank E.G. Rathjen for the anti-L1.

## COMPETING INTERESTS STATEMENT

The authors declare that they have no competing financial interests.

Received 18 June; accepted 15 July 2005

Published online at <http://www.nature.com/natureneuroscience/>

1. Lyuksyutova, A.I. *et al.* Anterior-posterior guidance of commissural axons by Wnt-frizzled signaling. *Science* **302**, 1984–1988 (2003).
2. Paxinos, G. *The Rat Nervous System* (Academic, New York, 1995).
3. Gianino, S. *et al.* Postnatal growth of corticospinal axons in the spinal cord of developing mice. *Brain Res. Dev. Brain Res.* **112**, 189–204 (1999).
4. Yoshikawa, S., McKinnon, R.D., Kokel, M. & Thomas, J.B. Wnt-mediated axon guidance via the *Drosophila* Derailed receptor. *Nature* **422**, 583–588 (2003).
5. Halford, M.M. *et al.* Ryk-deficient mice exhibit craniofacial defects associated with perturbed Eph receptor crosstalk. *Nat. Genet.* **25**, 414–418 (2000).
6. Joosten, E.A., Reshilov, L.N., Gispen, W.H. & Bar, P.R. Embryonic form of N-CAM and development of the rat corticospinal tract; immuno-electron microscopical localization during spinal white matter ingrowth. *Brain Res. Dev. Brain Res.* **94**, 99–105 (1996).
7. Zou, Y., Stoeckli, E., Chen, H. & Tessier-Lavigne, M. Squeezing axons out of the gray matter: a role for slit and semaphorin proteins from midline and ventral spinal cord. *Cell* **102**, 363–375 (2000).
8. Cohen, N.R. *et al.* Errors in corticospinal axon guidance in mice lacking the neural cell adhesion molecule L1. *Curr. Biol.* **8**, 26–33 (1998).
9. Castellani, V., Chedotal, A., Schachner, M., Faivre-Sarrailh, C. & Rougon, G. Analysis of the L1-deficient mouse phenotype reveals cross-talk between Sema3A and L1 signaling pathways in axonal guidance. *Neuron* **27**, 237–249 (2000).
10. Dottori, M. *et al.* EphA4 (Sek1) receptor tyrosine kinase is required for the development of the corticospinal tract. *Proc. Natl. Acad. Sci. USA* **95**, 13248–13253 (1998).
11. Arlotto, P. *et al.* Neuronal subtype-specific genes that control corticospinal motor neuron development *in vivo*. *Neuron* **45**, 207–221 (2005).
12. Dickson, B.J. Molecular mechanisms of axon guidance. *Science* **298**, 1959–1964 (2002).
13. Lu, W., Yamamoto, V., Ortega, B. & Baltimore, D. Mammalian Ryk is a Wnt coreceptor required for stimulation of neurite outgrowth. *Cell* **119**, 97–108 (2004).
14. Frohman, M.A., Boyle, M. & Martin, G.R. Isolation of the mouse Hox-2.9 gene; analysis of embryonic expression suggests that positional information along the anterior-posterior axis is specified by mesoderm. *Development* **110**, 589–607 (1990).
15. Hovens, C.M. *et al.* RYK, a receptor tyrosine kinase-related molecule with unusual kinase domain motifs. *Proc. Natl. Acad. Sci. USA* **89**, 11818–11822 (1992).
16. Serafini, T. *et al.* Netrin-1 is required for commissural axon guidance in the developing vertebrate nervous system. *Cell* **87**, 1001–1014 (1996).
17. Cheng, H.J. & Flanagan, J.G. Identification and cloning of ELF-1, a developmentally expressed ligand for the Mek4 and Sek receptor tyrosine kinases. *Cell* **79**, 157–168 (1994).

---

## Corrigendum: Protocadherin Celsr3 is crucial in axonal tract development

Fadel Tissir, Isabelle Bar, Yves Jossin, & André M Goffinet

*Nat. Neurosci.* **8**, 451–457 (2005)

In the print version of this article and the version initially published online, an author name was omitted. The fourth author should have been listed as Olivier De Backer of the Molecular Physiology Research Unit, University of Namur Medical School, 61, rue de Bruxelles, B5000 Namur, Belgium. The error has been corrected in the HTML and PDF versions of the article. This correction has been appended to the PDF version. The authors regret the error.

---

## Corrigendum: Ryk-mediated Wnt repulsion regulates posterior-directed growth of corticospinal tract

Yaobo Liu, Jun Shi, Chin-Chun Lu, Zheng-Bei Wang, Anna I Lyuksyutova, Xuejun Song & Yimin Zou

*Nat. Neurosci.* **8**, 1151–1159 (2005)

In the print version of this article and the version initially published online, one author's name was spelled incorrectly. The correct spelling is Xue-Jun Song. The error has been corrected in the HTML and PDF versions of the article. This correction has been appended to the PDF version. The authors regret the error.

---

## Corrigendum: Activity-dependent decrease of excitability in rat hippocampal neurons through increases in $I_h$

Yuan Fan, Desdemona Fricker, Darrin H Brager, Xixi Chen, Hui-Chen Lu, Raymond A Chitwood & Daniel Johnston

*Nat. Neurosci.* **8**, 1542–1551 (2005)

In the print version of this article and the version initially published online, the units for anisomycin concentration in the figure labels for Fig. 8d and f were incorrect. The correct concentration is 20  $\mu$ M. The error has been corrected in the HTML and PDF versions of the article. This correction has been appended to the PDF version. The authors regret the error.